Direct Observation of Spin Waves above T_C for Nickel

H. A. Mook
Solid State Division, Oak Ridge National Laboratory, Oak Ridge, Tennessee 37831

and

J. W. Lynn
Department of Physics, University of Maryland, College Park, Maryland 20742
(Received 17 March 1986)

Inelastic-neutron-scattering measurements with the constant-**q** technique have been used to characterize the energy response of the scattering in paramagnetic nickel. At small wave vectors **q**, the scattering peaks at zero energy, indicative of spin diffusion, but at larger **q** the scattering maximizes at finite $\pm E$ demonstrating that the spectral response has propagating character. The relative width $\Delta E/E$ of the excitation decreases with increasing $|\mathbf{q}|$ as expected, with the excitation becoming well defined as its energy becomes comparable with kT.

PACS numbers: 75.30.Ds, 75.50.Cc

A proper description of the magnetic excitations in isotropic ferromagnets such as nickel and iron is an important problem which continues to attract considerable interest both theoretically and experimentally. In particular the existence of propagating excitations in the paramagnetic phase of these materials, discovered in 1973,[1,2] has recently been questioned by Shirane and co-workers.[3,4] In the present Letter we report the results of extensive polarized- and unpolarized-neutron measurements on nickel, with the specific intention of establishing the nature of the energy response of the scattering. At small values of the wave vector **q** we find that the scattering is diffusive in nature, as is well known, while at larger q we find that the scattering displays a propagating character as previously reported.[1,2,5]

The measurements were carried out using the triple-axis neutron-scattering technique. Beryllium monochromator and analyzer crystals were employed for the unpolarized-beam measurements, while ^{57}Fe crystals were used for the polarized-beam data collection. Both types of crystals have small d spacings which yield naturally good resolution. The sample was a single crystal of ^{60}Ni weighing 403 g, which is more than three times the size of the sample used in our early measurements and sixteen times the size of the Brookhaven sample.[3,4] The large sample size, coupled with the dramatic advances in polarized-beam technology realized in the last fifteen years, has allowed us to make reliable measurements for the entire wave-vector range of interest, from small q where the scattering is strong, through the range of intermediate energies where the phonon scattering interferes with measurements of the magnetic response, into the high-energy range where E exceeds the ordering energy kT_C.

In general, polarized-beam data are preferred since an unambiguous measurement of the magnetic cross section can be made if the $\mathbf{H}\parallel\mathbf{Q}-\mathbf{H}\perp\mathbf{Q}$ technique is used. To obtain such data the intensity is measured with a small (~ 30 Oe) guide field parallel to the wave-vector transfer **Q**. In this configuration the neutron reverses its spin (spin-flip scattering) for scattering which is purely magnetic in origin, so that we obtain the magnetic response M (plus background). With $\mathbf{H}\perp\mathbf{Q}$, on the other hand, the magnetic (spin flip) scattering is only half as strong, so that we obtain $M/2$ (plus background). The difference then yields $M/2$, with a complete cancellation of background. However, the polarized-beam technique is limited by the signal-to-noise ratio of the data, which is typically more than an order of magnitude lower than with conventional unpolarized techniques. The unpolarized-beam technique relies on using very high resolution so that the single-phonon peaks and incoherent (elastic) scattering can be easily identified and isolated. Background was eliminated in this case by making measurements at the identical temperatures and wave vectors with the analyzer crystal rotated off reflection, and then subtracting these data from the data obtained with the analyzer reflecting. Of course with unpolarized neutrons there is no way to separate the magnetic cross section from other contributions to the scattering, such as from the furnace, multiphonon scattering, double scattering, etc.

For the present range of wave vectors and energies, the neutron-scattering cross section can be written in terms of an isotropic scattering function $S(q,E)$ as

$$S(q,E)\propto\chi(q)F_q(E)\frac{E/kT}{1-\exp[-(E/kT)]}. \quad (1)$$

The wave-vector-dependent susceptibility $\chi(q)$ is given approximately by $1/(\kappa^2+q^2)$, where the inverse correlation range κ is zero for $T\leq T_C$. The term containing E/kT is the thermal (detailed balance) factor. The spectral-weight function $F_q(E)$ is the function of primary interest since it describes the shape of the scattering as a function of energy, and is normalized to

unity when integrated over all energies. At small q the scattering is diffusive in nature above T_C, and $F_q(E)$ is often approximated by a single Lorentzian in energy centered at $E=0$,

$$F_q(E)=(1/\pi)[\Gamma/(\Gamma^2+E^2)], \quad (2)$$

although there are more accurate forms that should be used for detailed comparisons of theory with experiment in the critical region.[6] Here Γ is the width in energy of the scattering, which increases rapidly with q (for example, at T_C, $\Gamma=Aq^{5/2}$ with $A\approx 350$ meV-Å$^{5/2}$ for nickel[7]). Thus measurements at small q are relatively easy since the scattering is intense and is restricted to a small range of energies. Alternatively, with increasing q we expect the magnetic scattering to decrease in overall intensity while spreading out in energy, making measurements increasingly difficult.

The results of high-resolution polarized-beam measurements for three $\mathbf{q}$'s are shown in Fig. 1. The top two scans were taken with a fixed final energy of 40 meV while 60 meV was employed for the bottom scan. In both cases horizontal collimations of 40′ (FWHM) were used before and after the sample. The polarized-beam subtraction technique ensures that the observed intensity is magnetic in origin. The scans shown are the result of averaging many data sets, and the statistical errors are indicated by the error bars in each case. The range of accessible energies in these scans is determined by the geometry of the beam entering and exiting the guide-field magnet needed to maintain the $\mathbf{H}\parallel\mathbf{Q}$ condition.

In contrast to the diffusive behavior found at smaller q's, it is clear that the scattering is not peaked at $E\approx 0$ at these q's, and Eq. (2) is not appropriate.[8] Instead we have chosen to use a spectral-weight function of the double-Lorentzian form

$$F_q(E)=\frac{1}{2\pi}\left[\frac{\Gamma}{(E_q-E)^2+\Gamma^2}+\frac{\Gamma}{(E_q+E)^2+\Gamma^2}\right], \quad (3)$$

where E_q identifies the spin-wave energy at $\pm E$ and Γ is the spin-wave linewidth. The solid curves are least-squares fits of Eqs. (1) and (3), convoluted with the full four-dimensional instrumental resolution. The dashed curve show the fits using spin-diffusion theory [Eq. (2) with $A=350$ meV-Å$^{5/2}$], which works well for $q\lesssim[0.08,0.08,0.08]$. At these larger q's we see that the fits are better with the spin-wave form for the cross section, although the excitations are of course heavily damped in this crossover region. We remark that Eq. (3) is not the only form for the spin-wave cross section that gives an adequate fit to these data; detailed results for a variety of possible forms for $F(q,E)$ will be given elsewhere.

Figure 2 shows measurements for higher q values.

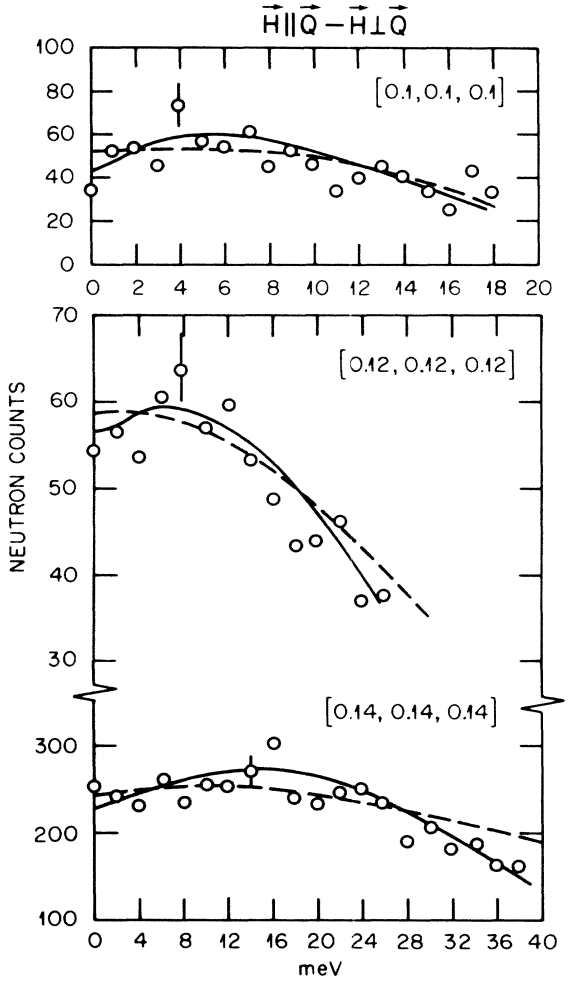

FIG. 1. Magnetic scattering at $1.06T_C$ obtained from polarized-beam measurements at three values of $\mathbf{q}$. The scattering maximizes at finite energy, rather than at $E\approx 0$ as it does at smaller values of q. The solid curves result from a fit to the data using the spin-wave cross section convoluted with the instrumental resolution. The spin-diffusion form for the cross section (dashed curves) does not fit these data as well.

The scattering is seen to peak at higher energies as expected, with the peaks in the scattering becoming better defined. In addition to the spin-wave side peaks we find small peaks at $E=0$ which appear to be resolution limited in width. The origin of this central peak is not known at present; however, its integrated spectral weight is very small compared to that of the spin-wave excitations. The solid curves shown are the same as for Fig. 1 except for the addition of this extra component, and give an excellent fit to the data. In contrast, the diffusive form for the cross section (dashed curves) is clearly inappropriate.

At still larger values of q the magnetic scattering decreases in intensity and thus becomes more difficult to measure. However, in this range of E and q the mag-

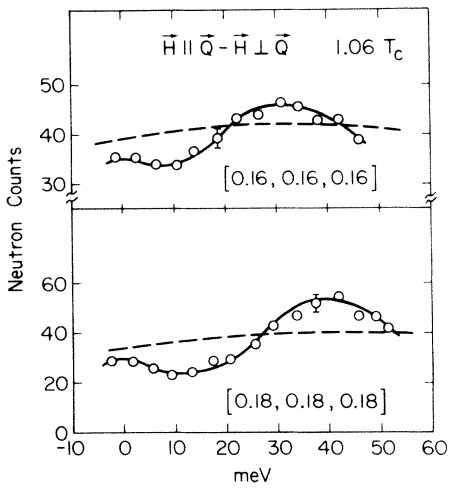

FIG. 2. Paramagnetic scattering at larger values of q obtained with the polarized-beam technique. Note that the maximum in the scattering shifts to higher energy with increasing q, while the relative width decreases. The diffusive form for the cross section (dashed curves) is clearly inappropriate.

netic scattering remains predominantly higher in energy than the phonon excitations, and hence we may employ unpolarized-beam measurements.[1,2] Figure 3 shows a high-resolution measurement for $\mathbf{q} = [0.2, 0.2, 0.2]$, taken with $E_f = 70$ meV and 20′ collimation before and after the sample. There is a large elastic peak ($E = 0$) which originates predominantly from the furnace and other sources of nonmagnetic scattering, and sharp excitations are observed for the transverse and longitudinal phonons. At higher energies we see a broad but easily observable spin-wave peak. Note that there is not much change in this scattering in going from 20 K below T_C to 20 K above T_C, as was found in the earlier work.[1,2]

The results of fitting Eqs. (1) and (3) to the data are shown in Fig. 4. The top portion gives the spin-wave energy as a function of q in the region where side peaks are observed in the raw data. We see that the energy increases rapidly with q as expected. Accompanied by the increase in excitation energy is a decrease in the relative energy linewidth as shown at the bottom. These results demonstrate conclusively that the scattering in nickel evolves in a continuous fashion from spin-diffusive behavior at small wave vectors, where Γ/E_{sw} exceeds a critical ratio R_c, to propagating character at larger wave vectors, where $\Gamma/E_{sw} < R_c$.[9] At this temperature the crossover occurs at $q \sim 0.3$ Å^{-1} while $\kappa = 0.9$ Å^{-1} so that we have $q > \kappa$ as expected. We believe that this scattering can be described most naturally in terms of propagating excitations, but a full interpretation must await a complete theoretical description of the dynamics of $3d$ itinerant paramagnets.

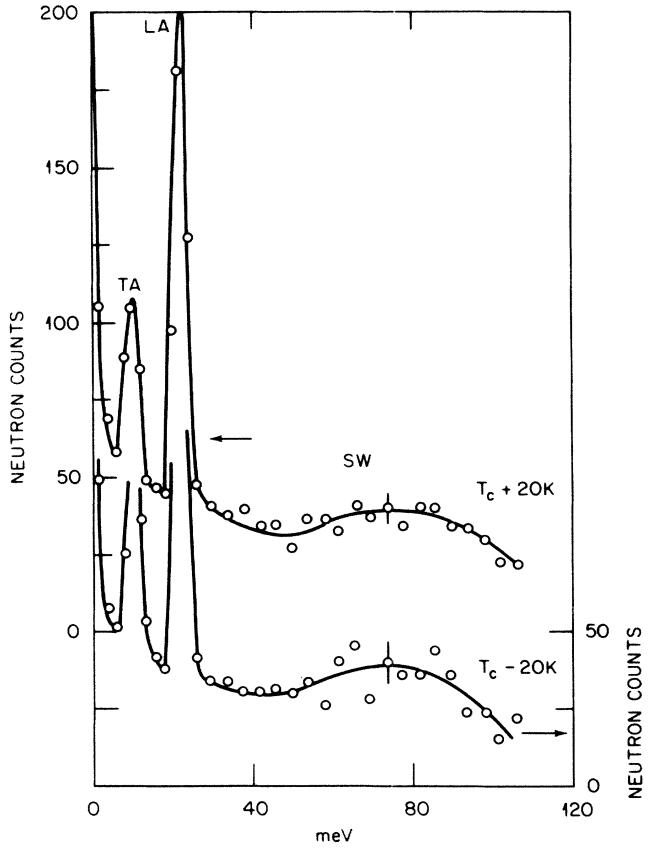

FIG. 3. Observed scattering with unpolarized neutrons at $\mathbf{q} = [0.2, 0.2, 0.2]$. The nuclear scattering dominates at low energies, while the broad magnetic spin-wave peak is evident at higher energies. Note that the magnetic scattering does not change dramatically in going from just below T_C to just above.

Finally we remark that caution should be exercised when comparing detailed theoretical line shapes with constant-$\mathbf{q}$ scans such as shown in Figs. 1–3. This is because when the scattering function $S(q,E)$ is very dispersive the instrumental resolution can substantially distort the intensity profiles when measured over large ranges of energy.[10] An alternate method of comparing theory and experiment, which has been used extensively for highly dispersive systems, employs the constant-E technique, which has the important advantage that the instrumental resolution does not change appreciably over the course of a measurement. An example of such a comparison is shown in Fig. 4, where we have plotted the observed maxima of constant-E scans for this system[1,2] (dashed curve) with the theoretical curve (dot-dashed) based on spin diffusion [Eqs. (1) and (2)]. It is clear that the spin-diffusion form for $S(q,E)$ does not represent the data well, as was shown originally,[1,2] and in more detail recently.[11] We note that since the dispersion surface $S(\mathbf{q},E)$ is broad, the maxima as measured in constant E and con-

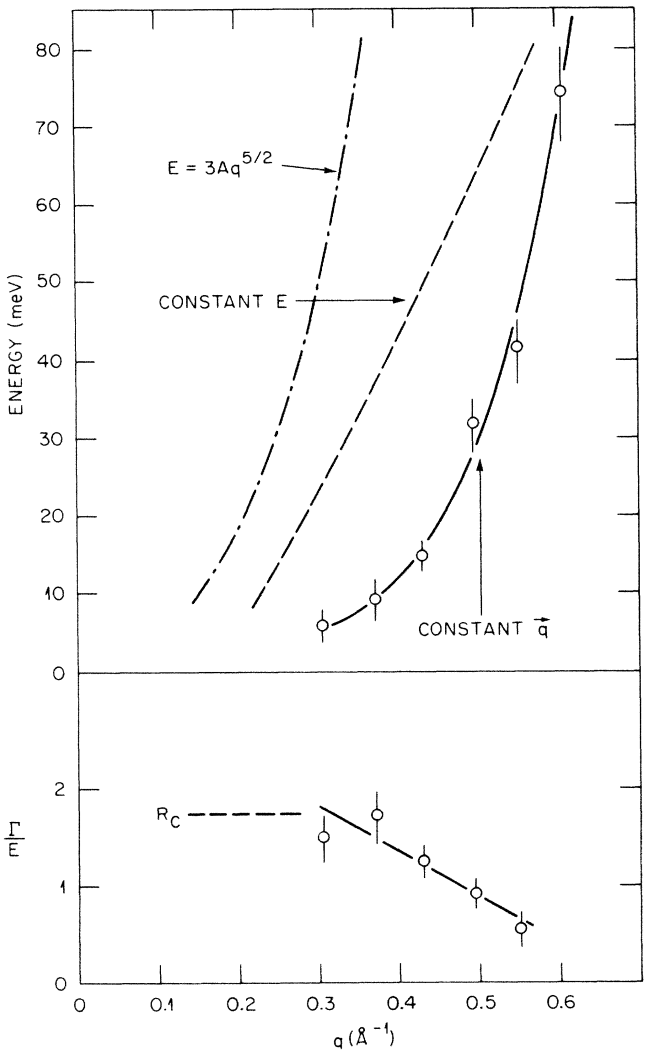

FIG. 4. The top portion shows the spin-wave energies above T_C as a function of q, obtained by fitting Eqs. (1) and (3) to the data. The position shifts rapidly to larger energy with increasing q as expected. The peak positions of $S(q,E)$ observed (Refs. 1 and 2) via the constant-E technique, which can be compared with theory more readily, are also shown (see text). The bottom portion displays the ratio of the linewidths to the excitation energies in the spin-wave region [defined as $\Gamma/E < (3)^{1/2}$]. The relative widths are seen to decrease rapidly with increasing q as the spin waves become better defined.

stant **q** *must* occur at different (**q**,E) (even when measured with perfect resolution) since they are taken along orthogonal paths. A simple example of this is given by the spin-diffusion formula, which has a maximum at $E \approx 0$ for constant **q** (at small q) while the constant-E peak occurs[11] at $E = 3Aq^{5/2}$ (at T_C) as shown in Fig. 4. Notice that the constant-E and constant-**q** maxima approach each other as Γ/E becomes small, as expected. Since the magnetic scattering can in principle be uniquely determined with polarized-beam techniques the entire scattering function can be established from high-resolution measurements using a closely spaced mesh of either constant-**q**, or constant-E scans.

Research at Oak Ridge National Laboratory was supported by the Division of Materials Sciences, U. S. Department of Energy under Contract No. DE-AC05-84OR21400 with Martin Marietta Energy Systems, Inc. Research at the University of Maryland was supported by National Science Foundation Division of Materials Research Contract No. 83-19936.

[1]H. A. Mook, J. W. Lynn, and R. M. Nicklow, Phys. Rev. Lett. **30**, 556 (1973).

[2]J. W. Lynn and H. A. Mook, Phys. Rev. B **23**, 198 (1981).

[3]G. Shirane, O. Steinsvoll, Y. J. Uemura, and J. Wicksted, J. Appl. Phys. **55**, 1887 (1984).

[4]O. Steinsvoll, C. E. Majkrzak, G. Shirane, and J. Wicksted, Phys. Rev. Lett. **51**, 2322 (1983).

[5]H. A. Mook and J. W. Lynn, J. Appl. Phys. **57**, 3006 (1985).

[6]B. I. Halperin and P. C. Hohenberg, Phys. Rev. **177**, 952 (1969); J. Hubbard, J. Phys. C **4**, 53 (1973).

[7]V. J. Minkiewicz, M. F. Collins, R. Nathans, and G. Shirane, Phys. Rev. **182**, 624 (1969).

[8]Recently J. L. Martinez, P. Boni, and G. Shirane [Phys. Rev. B **32**, 7037 (1985)] have reported polarized-beam measurements at [0.1, 0.1, 0.1] and [0.12, 0.12, 0.12]. Convolution of the present spin-wave cross-section parameters with their coarser resolution produces *no* side peaks at these q's, in agreement with their data.

[9]We can define the critical ratio to be the value where the spectral-weight function crosses over from a single peak (centered at $E = 0$) to a function with side peaks at $\pm E$. For Eq. (3), $R_c = (3)^{1/2}$.

[10]J. W. Lynn and H. A. Mook, Physica (Amsterdam) **136B**, 94 (1986).

[11]J. W. Lynn, Phys. Rev. Lett. **52**, 775 (1984).